

Accepted Manuscript

Title: TiO₂-sludge carbon enhanced catalytic oxidative reaction in environmental wastewaters applications

Author: Sunil Athalathil Boštjan Erjavec Renata Kaplan
Frank Stüber Christophe Bengoa Josep Font Agusti Fortuny
Albin Pintar Azael Fabregat



PII: S0304-3894(15)00554-3
DOI: <http://dx.doi.org/doi:10.1016/j.jhazmat.2015.07.025>
Reference: HAZMAT 16952

To appear in: *Journal of Hazardous Materials*

Received date: 9-4-2015
Revised date: 16-6-2015
Accepted date: 15-7-2015

Please cite this article as: Sunil Athalathil, Boštjan Erjavec, Renata Kaplan, Frank Stüber, Christophe Bengoa, Josep Font, Agusti Fortuny, Albin Pintar, Azael Fabregat, TiO₂-sludge carbon enhanced catalytic oxidative reaction in environmental wastewaters applications, *Journal of Hazardous Materials* <http://dx.doi.org/10.1016/j.jhazmat.2015.07.025>

This is a PDF file of an unedited manuscript that has been accepted for publication. As a service to our customers we are providing this early version of the manuscript. The manuscript will undergo copyediting, typesetting, and review of the resulting proof before it is published in its final form. Please note that during the production process errors may be discovered which could affect the content, and all legal disclaimers that apply to the journal pertain.

TiO₂-Sludge carbon enhanced catalytic oxidative reaction in environmental wastewaters applications

Sunil Athalathil^a, BoštjanErjavec^b, RenataKaplan^b, Frank Stüber^a, Christophe Bengoa^a, JosepFont^a, AgustiFortuny^c, AlbinPintar^{b*} and AzaelFabregat^{a*}

^aDepartament d'Enginyeria Química, ETSEQ, Universitat Rovira i Virgili, Av. Paisos Catalans 26, 43007. Tarragona, Catalunya, Spain

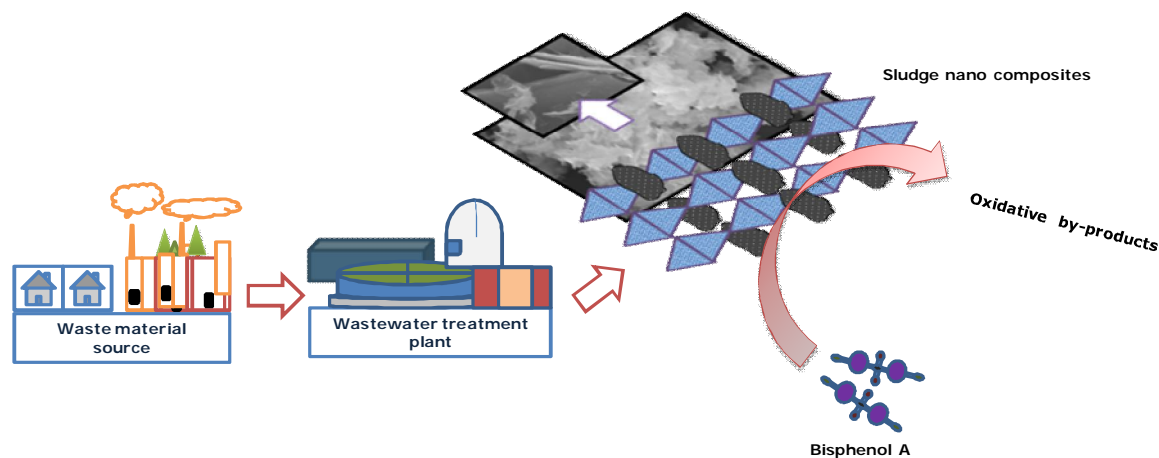
^bLaboratory for Environmental Sciences and Engineering, National Institute of Chemistry, Hajdrihova 19, SI-1001 Ljubljana, Slovenia

^cDepartament d'Enginyeria Química, EPSEVG, Universitat Politècnica de Catalunya, Av. Victor Balaguer s/n, 08800 Vilanova i la Geltru, Catalunya, Spain

* Corresponding authors: AzaelFabregat. Address: Departament d'Enginyeria Química, ETSEQ, Universitat Rovira i Virgili, Av. Paisos Catalans 26, 43007. Tarragona, Catalunya, Spain. Tel: + (34) 977559643. Fax: + (34) 977559667. E-mail : azael.fabregat@urv.cat

AlbinPintar. Address: Laboratory for Environmental Sciences and Engineering, National Institute of Chemistry, Hajdrihova 19, SI-1001 Ljubljana, Slovenia. Tel: +386 1 4760 237. E-mail: albin.pintar@ki.si

GRAPHICAL ABSTRACT



HIGHLIGHTS:

- Efficient sludge nanocomposites(SNCs) fabricated from sludge biomass.
- The SNCs enhanced BisphenolA removal.
- Surface modification processes displayed crystallinity and good surface textures.
- The presence of SNC-HD solid exhibit highest photocatalyticactivity.

ABSTRACT

The enhanced oxidative potential of sludge carbon/TiO₂nanocomposites (SNCs), applied as heterogeneous catalysts in advanced oxidation processes(AOPs), was studied. Fabrification of efficient SNCs using different methods and successful evaluation of their catalytic oxidative activity is reported for the first time. Surface modification processes of hydrothermal deposition, chemical treatment and sol-gel solution resulted in improved catalytic activity and good surface

chemistry of the SNCs. The solids obtained after chemical treatment and hydrothermal deposition processes exhibit excellent crystallinity and photocatalytic activity. The highest photocatalytic rate was obtained for the material prepared using hydrothermal deposition technique, compared to other nanocomposites. Further, improved removal of bisphenol A (BPA) from aqueous phase by means of catalytic ozonation and catalytic wet air oxidation processes is achieved over the solid synthesized using chemical treatment method. The present results demonstrate that the addition of TiO_2 on the surface of sludge carbon (SC) increases catalytic oxidative activity of SNCs. The latter produced from harmful sludge materials can be therefore used as cost-effective and efficient sludge derived catalysts for the removal of hazardous pollutants.

Keywords: sludge carbons; wastewater treatment; nano composites; fabrication process; catalytic oxidative reaction

1. Introduction

In recent years, titanium dioxide (TiO_2) nano materials have been successfully applied in many environmental treatment applications. TiO_2 nano materials have great practical importance due to their high stability, non toxicity, biocompatibility and useful properties for applications in photoreactions, semi conductors, solar cells and electro chemistry [1-2], but still suffer due to the low efficiency, high cost and short irradiation range. Generally, TiO_2 assisted nanomaterials are produced by different methods, including hydrothermal synthesis, chemical treatment, sol-gel solution and vapor phase deposition [3-6]. There have been many research reports of TiO_2 nano materials (e.g., nanotubes, nanowires, nanorods, nanofibres and nanoclusters) that exhibit high surface area, good surface textures and excellent catalytic activity [7-11].

A landmark review reported on the carbon-titanium based photocatalysts that are fabricated with various supporting materials, including activated carbon, fullerene (60) and graphene[12]. Among them, activated carbons (AC) perform better in several environmental treatment applications such as photoreaction, ozonation and heterogeneous catalyzed reactions [13]. Due to the economic benefits, many researchers have been gearing up on the development of cost-effective and low toxicity catalysts from waste biomass [14]. Only few studies have reported TiO₂ deposited on the activated carbons for the removal of hazardous pollutants from water and wastewaters [15-18]. Li et al. recently reviewed various aspects of titaniumdioxide supported activated carbon, including, preparation andmechanism of photo catalytic reaction [19]. The photo degradation of wastewater using TiO₂-AC fibers has reported [20]. Yu et al studied the adsorption and photo catalytic removal of azodye using TiO₂-carbon nanotubes [21].Doong and Chiang have reported the removal of organic compounds and heavy metals using titaniate-carbon nanotubes composites [22]. These activated carbon based nano materials have vouched for the cost-effective and good treatment methods to many environmental treatment applications.

On the other hand, the amount of sludge solid residues is increasing day by day due to the urbanization and industrialization, and such wastes are available at zero cost. These materials are rich in carbonaceous content, and consist of organic and inorganic compounds as well as small quantity of nutrients. Huge amounts of sludge waste materials cause disposal problems and are considered as one of the most costly and challengeable tasks in wastewater treatment plants (WWTPs) [23]. These sludge solid materials can be for instance converted into useful catalyst supporting materials that could be utilized for the treatment of hazardous compounds found in the environment.

In this study, sludge carbon/TiO₂ nano composites (SNCs) were fabricated using different preparation methods such as chemical treatment (CT), hydrothermal deposition (HD) and sol-gel solutions (SGS), and their catalytic activity was successfully evaluated in various advanced oxidation processes (AOPs) for water treatment, **such as catalytic ozonation, photocatalytic oxidation and catalytic wet air oxidation.**

BisphenolA (BPA) is an endocrine disrupting chemical (EDC) that has been extensively used in chemical industry, food industry and pharmaceutical applications. The EDCs once introduced into the aquatic environment exhibit high toxicity and estrogenic effects to living organisms [24-25]. In the present study, model BPA aqueous solution was treated by the above-mentioned AOPs utilizing the synthesized SNCs. The latter have shown high BET surface areas, and subsequently enhanced the catalytic oxidative removal of BPA. Additionally, the sludge carbon DS800 sample itself shows significant catalytic activity that was even further improved after a surface modification process. Based on these observations, one can produce a cheap and effective nano composite from the harmful sludge materials for the environmental treatment applications.

2. Experimental section

2.1 Fabrication of sludge nano composites

2.1.1 Preparation of DS800 sludge carbons

The slurry anaerobic sludge was dried in a furnace at 105 °C for 24 h. This material was soaked in distilled water for 2 h and dried at 105 °C for 48 h. The resulting dried sludge (DS) material was grinded and sieved approximately to mesh size ranges from 0.5 to 0.7 mm. 10 g of dried sludge was placed in a quartz reactor (AFORA, Ref no: V59922) and carbonized at 800 °C for a

fixed dwell time of 2 h. This material was washed several times with distilled water and then grinded to very fine powder using a mortar and pestle. The powder sludge carbon was denoted as DS800. The weight ratio of DS800 and TiO_2 was maintained at 1:1 for all the fabrication processes.

2.1.2 *Chemical treatment*

DS800 (1.0 g) and 1.0 g of TiO_2 P25 Degussa (Sigma-Aldrich) was added to 150 mL of 10 mol/L NaOH solution, then the solution was thoroughly mixed with ultrasonic homogenizer for 10 min. The solution was placed in a Teflon-lined autoclave, and hydrothermally treated at 130 °C for 24 h. The solid was cooled and divided into two equal portions. The first portion was washed several times with Milli-Q water. The second portion was washed three times with 0.1 mol/L Hydrochloric acid solution and thoroughly washed with Milli-Q water. The final materials were separated by centrifugation and freeze-dried.

2.1.3 *Hydrothermal deposition*

1.0 g of DS800 and 3.45 g of $\text{TiOSO}_4 \cdot \text{H}_2\text{SO}_4 \cdot \text{H}_2\text{O}$ (Sigma-Aldrich) were mixed in 100 mL of Milli-Q water. The solution was thoroughly mixed with ultrasonic homogenizer for 10 min and then the sample was placed in the Teflon-lined autoclave for 5 hours at 120 °C. The obtained materials were thoroughly washed with Milli-Q water followed by centrifugation and the obtained material was dried at 80 °C in air for 12 h.

2.1.4 *Sol-gel solutions*

66.8 mL of isopropanol (Sigma-Aldrich) was added to a 250 mL RB flask and then 3.70 mL of $\text{Ti}[\text{OCH}(\text{CH}_3)_2]_4$ (Merck) solution was carefully added drop wise to the mixture at vigorous

stirring conditions. Equal volume of water/nitric acid (65 %, Sigma-Aldrich) solution was added drop wise to the mixture and refluxed at 80 °C under vigorous stirring for 60 min. After the formation of a white precipitate 1.0 g of DS800 was added. This suspension was stirred at room temperature for 180 min. The obtained material was separated by means of centrifugation and dried at 80 °C in air for 12 h. To obtain the sludge nano composites, all the fabricated materials were further calcinated at 300 °C in air for 60 min.

2.2 Characterization of nano composites

Micro structure images of nano composites were determined using scanning electron microscope (SEM) and transmission electron microscopy (TEM). Elemental compositions of the nano composites were analyzed by energy dispersive X-ray (EDX) spectrum (Inca system, Oxford instruments) instrument. The **Fourier transform infrared spectroscopy** (FTIR) spectra were recorded in **Attenuated Total Reflectance**(ATR) mode by using a Perkin Elmer spectrometer (model Frontier) in the frequency range between 4000 to 400 cm^{-1} . The surface area of materials was determined by measuring nitrogen adsorption and desorption isotherms at -196 °C (Micromeritics, model Tristar II 3020). BET (Brunauer–Emmett–Teller) theory was applied in order to calculate the specific surface area of materials. **X-ray diffraction**(XRD) diffractograms were obtained using a D/max-ra X–ray diffract meter (Bruker-AXS D8- Discover diffractometer) with CuK radiation at 40 kV and 40 mA over the 2θ range of 5-70°. Diffuse reflectance UV–Vis spectra were obtained using a Perkin-Elmer Lambda 35 spectrophotometer equipped with the RSA-PE-19M Praying Mantis accessory. BPA conversions were monitored using a HPLC instrument (Spectra SystemTM), which operated in the isocratic analytical mode using 100 mm \times 4.6 mm BSD Hypersil C12 2.4 μm column with the flow rate of 0.5 mL/min and methanol: ultrapure water of 70:30 (UV detection at $\lambda = 210$ nm).

2.3. Catalytic activity measurements

2.3.1. Ozonation reaction

Ozonation reaction was carried out in a batch reactor thermostated at 15 °C. The ozone/oxygen mixture was used and flow was adjusted to 40 mL/min. 100 mg of SNCs material was homogeneously dispersed in 500 mL of BPA solution ($C_0=10$ mg/L) by an ultrasonic homogenizer for 2 min. Before starting the experiment, the solution was stirred for 20 min in order to avoid the initial adsorption effect of the nano composites.

2.3.2. Photocatalytic reaction

For the photocatalytic reaction, 31.3 mg of SNCs was dispersed in 250 mL of BPA solution. The reactor unit was thermostated at $T = 20$ °C (Julabo, model F25), magnetically stirred (300 rpm) and continuously sparged with purified air (45 L/h). **Initially, the mixture of solution was stirred for 30 min (dark time) in order to establish the equilibrium of the sorption process.** The photocatalytic oxidation was carried out under the **UV high-pressure mercury lamp (150 W, with a maximum λ at 365 nm)** irradiation for 60 min.

2.3.3. Catalytic wet air oxidation

The catalytic wet air oxidation experiments were performed in a continuous-flow trickle-bed reactor with catalyst loading of 300 mg at 200 °C, total pressure of 25.5 bar and oxygen partial pressure equal to 10 bar. The aqueous solution of BPA ($C_{\text{feed}} = 10$ mg/L) was fed ($Q_{\text{vol.}} = 0.5$ mL/min) into the reactor unit by means of HPLC positive alternative displacement pump (Gilson, model 307). Liquid-phase samples were collected at the reactor outlet by an automated sampler at the regular time intervals, and the duration of the experiment was set to about 40 h.

3. Results and discussion

3.1. Surface textures of nano composites

The fabricated SNCs were characterized using advanced techniques in order to examine their structural configurations and morphologies. The micro structure of nano composites was determined by scanning electron microscopy (SEM) and transmission electron microscopy (TEM). The micro structure images of SNCs are presented in **Figure 1**. The surface of SNCs was not uniform; further, they were highly impacted by the surface modifications process. **Figures 1 A and B** show the SEM images of SNCs prepared via chemical treatment (CT) through the water and acid washing, denoted as (SNC-CT-W) and (SNC-CT-A), respectively; feather like nanostructures with small bundle shape were obtained. The observation shows that the surface of SNCs remains with little changes in the special arrangement after the acid washing process. The structure of SNC-CT-A sample (**Figure 1 B**) confirms that the TiO_2 particle aggregates have densely appeared around the sludge carbon (SC) surface. On the images 3D flower like structures are observed. TEM images of SNCs are shown in **Figure 1**.

TEM images of SNC-CT-W (**Figure 1 A2, A3**) and SNC-CT-A (**Figure 1 B2, B3**) samples show the dark spots with spindle shape covered throughout the surface. The formation of SNCs using chemical treatment forms 3D flower like structures and a facial arrangement is clearly visible. The impurities of sludge carbon and amorphous carbon are also observed.

(Figure 1)

Hydrothermally deposited materials (denoted as SNC-HD) exhibit small granular particle size that are thickly arranged in surface. Similar composites were also obtained using the sol-gel solution method. The growth of TiO_2 particles was not homogeneous in the SNCs. It can be

concluded that the fabrication methods as well as precursors considerably influence the properties of SNCs[26].

The SEM images of SNC-HD sample (**Figure 1 C**) show hard grained clusters and consist of many ball-shaped nanoparticles over the surface. They are mostly nano particle sized and clearly observed on the TEM image (**Figure 1 C2 & C3**). The SEM images of sol-gel developed SNCs, denoted as SNC-SG, are shown in **Figure 1 D**. They show small ball-shaped size and densely arranged surface (**Figure 1 D2 & D3**).

To obtain the sludge carbon DS800, sewage sludge was calcinated in the absence of air at 800 °C for 2 h. The derived DS800 solid has hard surface and shows pores of different size, which can hinder mass transfer and consequently decrease catalytic activity. The surface images of sludge carbon (DS800) are shown in **Figure 1S**.

(Figure 1S)

Since the DS800 is originated from sewage sludge, it also contains impurities like organic, inorganic and volatile compounds. EDX spectral analysis detected the elemental fraction of the nano composites, which are mainly composed of **TiO₂ and SC**.The detection of metallic **titanium** fails in the SNC-SG material (**Figure 2S**), while lower amount of **titanium** was observed in the SNC-HD solid.

(Figure 2S)

This is probably because of the growth mechanism of titanium particles utilizing the concerned methods. On the contrary, high amount of titanium particles was detected for chemically treated sludge nano composites.

The microcrystallinity of the SNCs was determined using XRD analysis, and the derived diffractograms are shown in **Figure 1**. The CT-W and CT-A materials (**Figure 1** A1 & B1) are composed mostly of rutile crystalline phase, and higher amount of anatase phase was observed for the hydrothermally deposited solid (**Figure 1** C1). In the case of sol-gel sample less anatase crystalline phase was found (**Figure 1** D1). The peaks at 25.4° correspond to the plane of anatase phase in the SNC-HD solid. The peaks of rutile phase were detected at 27.5° for CTs samples. The XRD examination of DS800 reveals the presence of amorphous carbon. Higher content of quartz (26.8°), calcite (29.5°) and a lower amount of albite (28°) were detected in the DS800 sludge carbon (**Figure 1S** A1).

Results of surface porosity of SNCs are presented in **Table 1**. The BET specific surface area and porosity were dramatically improved using different modification processes. BET specific surface area of SNC-HD material ($309 \text{ m}^2/\text{g}$) was quite higher in comparison to other SNCs. Lower BET surface area was measured for the SNC-CT-W material ($3.0 \text{ m}^2/\text{g}$), which is probably due to the sodium salts accumulated in the pore cavities. Physiochemical properties such as surface area, crystallinity and functional groups were enhanced the oxidative catalytic reactions[27].

(Table 1)

The surface porosity of the samples fabricated using hydrothermal and a sol-gel solution process is highly enhanced. The total pore volume of nano composites was in the range of $0.01\text{-}0.39 \text{ cm}^3/\text{g}$. The pore diameters of SNCs were in the range of $2.9\text{-}22.1 \text{ nm}$. Better porosity and the higher surface area could enhance the adsorption of BPA molecule.

The UV-Vis diffuse reflectance spectra of SNCs are shown in **Figure 2 A**. These results were almost similar, but quite different from spectra of DS800 sludge carbon and commercial TiO₂ P25 sample. The SNCs exhibit an intense absorbance below 350-400 nm. The absorbance spectra of SNCs reasonably show a combination of features seen in the spectra of DS800 sludge carbon and TiO₂ P25 (commercial sample from Degussa) nano particles.

FTIR/ATR spectra illustrated in **Figure 2 B** give information about functional groups present on the surface of solids. The main vibrations for sludge carbon DS800 are observed at 1000 cm⁻¹, which is related to Si-O vibration. Another major peak is observed at 1500 cm⁻¹ for the SNCs material that could be attributed to stretching of aromatic compounds. The band at 1612 cm⁻¹ appeared for SNCs, which is related to vibration of quinone and -C=O group. There are two peaks (in the range of 1000-1300 cm⁻¹) observed for SNCs associated to C-O stretching band of ethers. After the treatment process, oxygenated functional groups peaks are significantly reduced. The chemical groups present in the SNCs are mostly belonging to aromatic and aliphatic compounds.

(Figure 2)

The nitrogen adsorption/desorption isotherms of SNCs are shown in **Figure 2C**. It can be seen that the SNCs follow hysteresis cycles that are closely related to type IV adsorption isotherms. The SNC-HD isotherms are quite different from the other fabricated materials, since they exhibit a large hysteresis loop, associated to meso porosity.

The results of thermal reduction of SNCs are shown in **Figure 3**. This thermal study leads to an observation that novel SNCs had better thermal stability, which was further supported by the results obtained in the continuous-flow catalytic wet air oxidation process conducted at elevated

temperature. The higher weight loss for DS800 sludge carbon was observed at 500 °C. The major weight loss for the SNC-CT-A solid was observed at 450 °C (**Figure 3 C**). A weak weight loss was also observed at 550 and 500 °C for SNC-HD (**Figure 3 D**) and SNC-SG (**Figure 3 E**) samples, respectively. The weight losses are mainly attributed to the removal of surface adsorbed compounds and their derivatives in the SNCs. **Based on the surface texture results indicate that there is a strong interaction of titanium oxide and sludge carbon. Our findings are supported with the results reported [28-29].**

(Figure 3)

3.2. Environmental wastewaters applications

3.2.1 Photocatalytic reaction

Figure 4A shows the photocatalytic activity of SNCs and sludge carbon for the removal of BPA from aqueous solution. Under the photoreaction in a period of 60 minutes, the SNC-HD particles were able to remove nearly 36 % of BPA from the solution. Photocatalytic activity of SNC-HD solid was obviously higher than of other nano composites.

(Figure 4)

BPA removal rate by using DS800 sludge carbon was very low compared to the other SNCs. DS800 material is obviously not a self-photocatalytic material under the UV irradiation range. The photoactivity of SNC-SG and SNC-CT-A materials was low, probably due to the lack of electron exchange over the sludge carbon matrix. Complete BPA removal in the presence of TiO₂ P25 sample was observed in the same period (**Figure 3S**).

(Figure 3S)

Only 27 % of BPA removal was measured over the SNC-CT-W solid. The results revealed that the SNC-HD material was the best candidate for the photocatalytic removal of emerging pollutant. The observation that the hydrothermal deposition conditions lead to the formation of more anatase phase, might favor the photocatalytic reaction[16].

The surface textures of the nano composites play a major role in the photocatalytic oxidation of BPA in the reactor system. Enhancement of photocatalytic activity of SNCs under UV light can be due to the surface chemistry, surface area, presence of oxygen and functional groups, such as quinone and carbonyl (detected in the FTIR/ATR spectra). On the basis of above surface characteristic information, a possible photocatalytic mechanism of SNCs could be proposed. It is suggested that the complex SNCs materials provide the **sludge carbon-titanium oxide** linkage that extends the photocatalytic activity[15]. The specific characteristics of the SNCs enable that (i) the sludge carbon serves as an electron carrier, and (ii) the number of holes and positive charge build on TiO_2 surface[30]. The electron carrier effects of SC contribute to avoid the recombination of photoelectrons and valence-band holes, which in turn enhances the formation of hydroxyl radicals and oxidation of liquid-dissolved BPA molecules. A mixture of SNCs and BPA solution was initially run in dark for 30 min, and no observable decrease of BPA concentration by adsorption was detected. This means that SNCs solids serve as photocatalysts to enhance BPA removal. **Figure 4B** shows the schematic illustration of photocatalytic reaction mechanism using SNCs.

3.2.2. Catalytic ozonation reaction

Figure 5A shows the removal of BPA in catalytic ozonation with SNCs and TiO_2 nano particles. SNC-HD and SNC-CT-W materials enabled complete removal of BPA during the 60 min

ozonation reaction. Complete BPA removal was achieved as well in the presence of commercial TiO₂ P25 sample. In a short period of 5 min high BPA removal of 75, 71 and 67 % was achieved for SNC-CT-A, SNC-CT-W and SNC-HD samples, respectively. While using TiO₂ P25, SNC-SG and DS800 samples, these values were equal to 61, 57 and 49 %, respectively, in the same time period (**Figure 5B**).

(Figure 5)

The SNCs as ozonation catalysts are shown to be more active in the removal of BPA from the liquid phase. SNCs with basic surface properties and with large pores enhanced this ozonation process. Suspensions of SNCs accelerate the decomposition of ozone, acting as initiators for the chain reaction and the transformation of the ozone molecules into secondary oxidants, which can react with adsorbed BPA molecules to form end products (**Figure 5C**). The surface textures of the SNCs play an important role in the ozonation of BPA solution. The adsorption of BPA solution could be strongly affected by the surface charge of nano composites[31].

3.2.3. Catalytic wet air oxidation

Figure 5D shows BPA conversions as a function of time on stream obtained in the presence of SNCs examined in the continuous-flow catalytic wet air oxidation (CWAO) process. Removal of BPA in the presence of SNC-CT-A solid was 96.4 %. For comparison, removal of BPA was 94.2 and 94.1 % for SNC-HD and SNC-SG samples, respectively. About 45 % BPA removal was measured using low surface area silicon carbide (SiC) as a reference inert material (**Figure 4S**), which is in good agreement with the results reported [32].

(Figure 4S)

This finding confirms that in the given range of experimental conditions BPA oxidation undergoes both catalyzed as well as non-catalyzed oxidation routes. Further, high BPA removal was attained using SNC-CT-A solid, compared to other materials. Based on this observation, the presence of oxygenated groups in the SNCs and continuous sparging with oxygen (O_2) accelerate the formation of hydroxyl radicals (HO^*), which can activate the BPA aromatic ring in order to form end products. **Figure 5E** shows the schematic illustration of catalytic wet air oxidation. Our new findings permit to imagine future research using products coming from the harmful waste solids. The biggest strength of this research work is to utilize zero cost waste solids for the removal Bisphenol-A by using advanced oxidation processes including, photocatalytic, catalytic ozonation and catalytic wet air oxidation in order to obtain biodegradable products at environmental acceptable conditions.

4. Conclusions

In summary, surface modification processes of hydrothermal deposition, chemical treatment and sol-gel solution resulted in improved catalytic activity and good surface chemistry of the SNCs. Materials obtained after chemical treatment and hydrothermal deposition processes displayed crystallinity and photocatalytic activity. In this study, better removal of BPA was achieved over the SNC-CT-A material in the catalytic ozonation and catalytic wet air oxidation reaction. The highest photocatalytic efficiency was achieved in the presence of SNC-HD solid, compared to other materials. Based on these observations, one can conclude that the addition of TiO_2 on the surface of sludge carbon (SC) increases the mobility of charges, electro negativity and electro affinities, which in turn enhances (photo)catalytic activity of these solids. Since the SNCs are produced from harmful sludge materials, they can be therefore used as cost-effective and

efficient biomass derived catalysts for the removal of hazardous pollutants from water and wastewaters.

Acknowledgements

A.P. and A.F. contributed equally to this research work. Use of facilities at the Laboratory for Environmental Sciences and Engineering, National Institute of Chemistry, Ljubljana, Slovenia, is acknowledged. A.P. acknowledges the financial support of the Ministry of Education, Science and Sport of the Republic of Slovenia through Research program P2-0150. A.F. acknowledges the financial support for this research that was provided by the Spanish Ministerio de Educación y Ciencia and FEDER, projects CTM2008-03338 and CTM2011-23069 from the Universitat Rovira i Virgili (Tarragona, Spain), for the financial support (2010BRDI/06–35). The author's research group is recognised by the Comissionat per a Universitats i Recerca del DIUE de la Generalitat de Catalunya (2009SGR865) and supported by the Universitat Rovira i Virgili (2010PFR-URV-B2-41).

References

- [1] Chen, X., Mao, S.S., 2007. Titanium dioxide nanomaterials: synthesis, properties, modifications and applications. *Chem. Rev.* 107 (7), 2891-2959.
- [2] Deng, D., Kim, M.G., Lee, J.Y., Cho, J., 2009. Green energy storage materials: Nanostructured TiO₂ and Sn-based anodes for lithium-ion batteries. *Energy Environ. Sci.* 2 (8), 818-837.
- [3] Kasuga, T., Hiramatsu, M., Hoson, A., Sekino, T., Niihara, K., 1999. Nanotubes Prepared by Chemical Processing. *Adv. Mater.* 11, 1307-1311.

- [4] Kajitvichyanukul, P., Ananpattarachai, J., Pongpom, S., 2005. Sol-gel preparation and properties study of TiO₂ thin film for photocatalytic reduction of chromium(VI) in photocatalysis process. *Sci. Tech. Adv. Mater.* 6 (3-4), 352-358.
- [5] Jitianu, T., Cacciaguerra, A., Benoit, R., Delpoux, S., Beguin, F., Bonnamy, S., 2004. Synthesis and characterization of carbon nanotubes–TiO₂nanocomposites. *Carbon.* 42, 1147-1151.
- [6] Kushibhatla, S.V.N.T., Karakoti, A.S., Bera, D., Seal, S., 2007. One dimensional nanostructured materials. *Prog. Mater. Sci.* 52 (5), 699-913.
- [7] Agatino Di Paola, Elisa García-López, Giuseppe Marcì, Leonardo Palmisano, 2012. Review: A survey of photocatalytic materials for environmental remediation, *J. Hazard. Mater.* 211–212, 3– 29.
- [8] Woan, K., Pyrgiotakis, G., Sigmund, W., 2009. Photocatalytic Carbon-Nanotube–TiO₂ Composites. *Adv. Mater.* 21 (21), 2233-2239.
- [9] Ebbesen, T.W., Lezec, H.J., Hiura, H., Bennett, J.W., Ghaemi, H.F., Thio, T., 1996. Electrical conductivity of individual carbon nanotubes. *Nature.* 382, 54-56.
- [10] Tong, H., Ouyang, S., Bi, Y., Umezawa, N., Oshikiri, M., Ye, J. H., 2012. Nano-photocatalytic materials: possibilities and challenges. *Adv. Mater.* 24 (2), 229-251.
- [11] Wu, H.B., Hng, H.H., Lou, X.W., 2012. Direct Synthesis of Anatase TiO₂ Nanowires with Enhanced Photocatalytic Activity. *Adv. Mater.* 24 (19), 2567-2571.

- [12] Leary, R., Westwood, A., 2011. Carbonaceous nonmaterial's for the enhancement of TiO₂photo catalysis- Review. Carbon. 49, 741-772.
- [13] W. Daud, W.M.A., Houshamnd, A.H., 2010. Textural characteristics, surface chemistry and oxidation of activated carbon.J. Natural Gas Chemistry.19, 267-279.
- [14] Smith, K.M., Fowler, G.D., Pullket, S., Graham, N.J.D., 2009. Sewage sludge-based adsorbents: A review of their production, properties and use in water treatment applications. Water.Res. 43, 2569-2594.
- [15] Matos, J., Laine, J., Herrmann, J.M., 1998. Synergy effect in the photocatalytic degradation of phenol on a suspended mixture of titania and activated carbon. Appl. Catal.B. 18, 281-291.
- [16] Liu, S.X., Chen, X.Y., Chen, X., 2007. A TiO₂/AC composite photo catalyst with high activity and easy separation prepared by a hydrothermal method.J. Hazard. Mater. 143, (1-2), 257-263.
- [17] Ou, H.H., Liao, C.H., Liou, Y.H., Hong, J.H., Lo, S.L., 2008. Photocatalytic oxidation of aqueous ammonia over microwave-induced titanate nanotubes. Environ. Sci. Technol. 42 (12), 4507-4512.
- [18] Kim, S., Kim, M., Hwang, S.H., Lim, S.K., 2012. Enhancement of photocatalytic activity of titania–titanate nanotubes by surface modification.Appl. Catal. B. (123-124), 391-397.
- [19] Li, P.G.,Awang, B., Duduku, K, Joseph, G.C., 2008. Preparation of titanium dioxide photocatalyst loaded onto activated carbon support using chemicalvapor deposition: A review paper. J. Hazard. Mater.157 (2–3), 209–219.

- [20] Yuan, R., Guan, R., Liu, P., Zheng, J., 2007. Photocatalytic treatment of wastewater from paper mill by TiO₂ loaded on activated carbon fibers. *Colloids Surf A*. 293 (1–3), 80–6.
- [21] Yu, Y., Yu, J.C., Chan, C.Y., Che, Y.K., Zhao, J.C., Ding, L., 2005. Enhancement of adsorption and photocatalytic activity of TiO₂ by using carbon nanotubes for the treatment of azodye. *Appl Catal B*. 61(1–2), 1–11.
- [22] Doong, R.A., Chiang, L.F., 2008. Coupled removal of organic compounds and heavy metals by titanate/carbon nanotube composites. *Water Sci Technol*. 58 (10), 1985–92.
- [23] Nassar, A.M., Mciwem, M.S., Afifi, S., 2009. Palestinian experience with sewage sludge utilizing reed beds. *Water Environ. J*. 23, 75–82.
- [24] Kuch, H.M., Ballschmiter, K., 2001. Determination of endocrine-disrupting phenolic compounds and estrogens in surface and drinking water by HRGC-(NCI)-MS in the picogram per liter range. *Environ. Sci. Technol*. 35 (15), 3201–3206.
- [25] Furhacker, M., Scharf, S., Weber, H., 2000. Bisphenol A: emissions from point sources. *Chemosphere*. 41 (5), 751–756.
- [26] Wang, X., Hu, Z., Chen, Y., Zhao, G., Liu, Y. and Wen, Z. 2009a. A novel approach towards high performance composite photocatalyst of TiO₂ deposited on activated carbon. *Appl. Surf. Sci*. 255 (7), 3953–3958.
- [27] Wang, K.H., Hsieh, Y.H., Wu, C.H., Chang, C.Y., 2000. The pH and anion effects on the heterogeneous photocatalytic degradation of o-methylbenzoic acid in TiO₂ aqueous suspension. *Chemosphere*. 40 (4), 389–94.

- [28] Matos, J., Laine, J., Herrmann, J.M., Uzcategui, D., Brito, J.L. 2007. Influence of activated carbon upon titania on aqueous photocatalytic consecutive runs of phenol photodegradation. *ApplCatal B*.70, 461–469.
- [29] Amjad, H. El-S., Alan, P. N., Hafid, Al-D., Suki, P., Neil, C., Steven, Y., 2004. Deposition of anatase on the surface of activated carbon. *Surf Coat Tech*. 187, 284–292.
- [30] Amy L. Linsebigler, Guangquan. Lu, John T. Yates, 1995. Photocatalysis on TiO₂ Surfaces: Principles, Mechanisms, and Selected Results. *Chem. Rev.* 95 (3), 735–758.
- [31] Guiza M, Ouerdeni A, Ratel A. 2004. Decomposition of dissolved ozone in the presence of activated carbon: An experimental study. *Ozone SciEng*.26(3), 299-307.
- [32] Erjavec, B., Kaplan, R., Djinović, P., Pintar, A., 2013. Catalytic wet air oxidation of bisphenolA model solution in a trickle-bed reactor over titanate nanotube-based catalysts. *Appl. Catal. B*. 132-133, 342-152.

FIGURES CAPTIONS

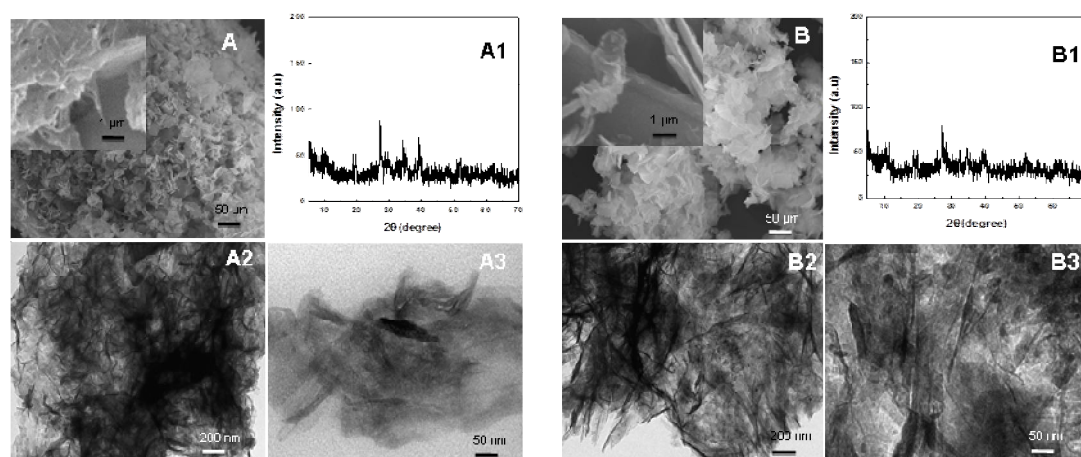
Figure 1. Scanning electron microscope (SEM) images of sludge nano composites fabricated using different fabrication methods: chemical treatment after the washing with water (A), acid (B), hydrothermal deposition (C), and sol-gel solution (D). X-ray diffraction (XRD) patterns of sludge nano composites chemically treated after washing with water (A1), acid (B1), hydrothermal deposition (C1) and sol-gel solution (D1). TEM images of sludge nano composites fabricated using chemical treatment after washing with water (A2 & A3), acid (B2 & B3), hydrothermal deposition (C2 & C3) and sol-gel solution (D2 & D3).

Figure 2. (A) UV-Vis diffuse reflectance spectra, (B) FTIR/ATR spectra, and (C) nitrogen adsorption/desorption isotherms of fabricated sludge nano composites, sludge carbon DS800 and TiO₂ P25 (Degussa).

Figure 3. Thermal reduction of sludge nano composites and sludge carbon DS800.

Figure 4. (A) Removal of BPA over sludge nano composites and sludge carbon DS800 during the period of 60 min under UV light; (B) schematic illustration of photocatalytic reaction mechanism using fabricated sludge nano composites.

Figure 5. (A) Ozonation reaction after 5 min using fabricated sludge nano composites, sludge DS800 and P25 TiO₂; (B) temporal course of ozonation reaction during the 60 min; (C) the schematic representation of catalytic ozonation reaction mechanism; (D) removal of BPA in the presence of sludge nano composites and sludge carbon DS800 obtained in the continuous-flow catalytic wet air oxidation reaction carried out in the trickle-bed reactor; (E) the schematic illustration of catalytic oxidation reaction mechanism.



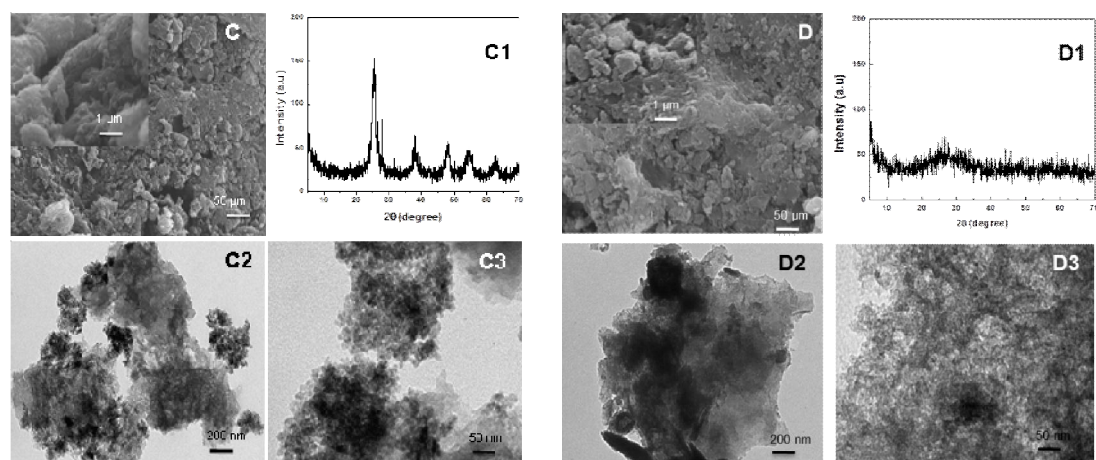
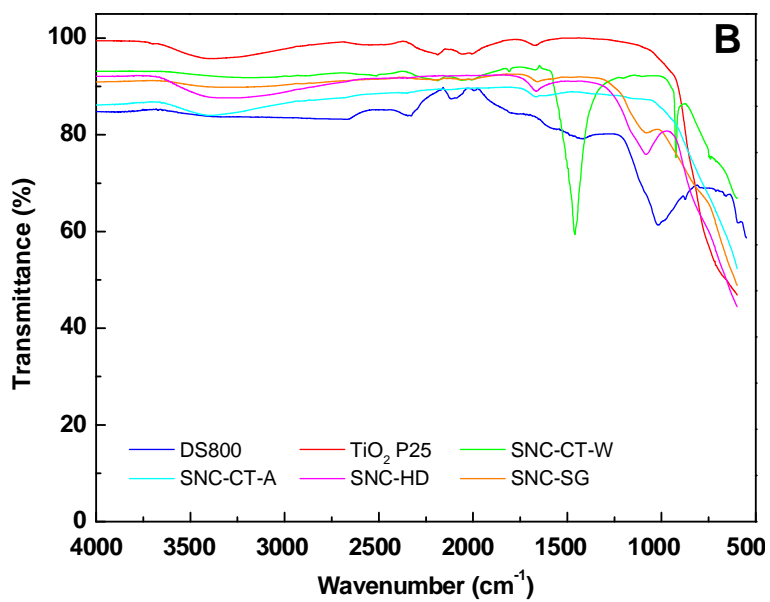
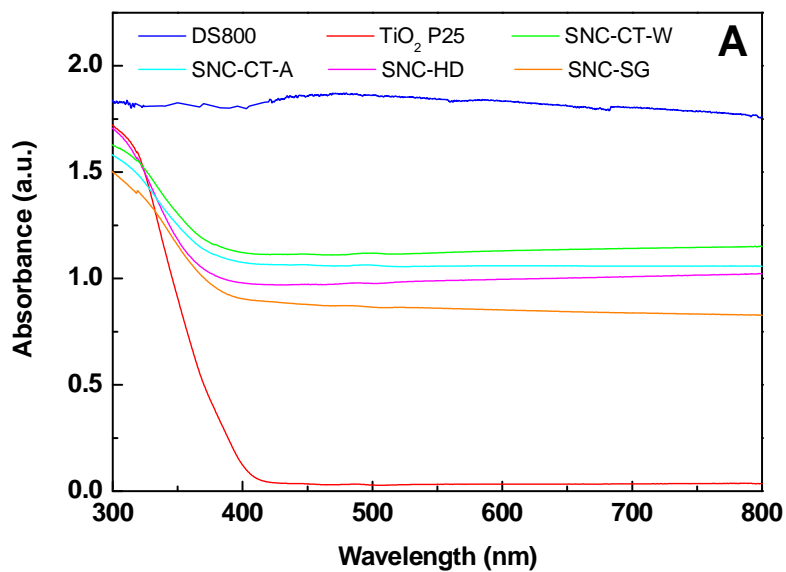


Figure 1.



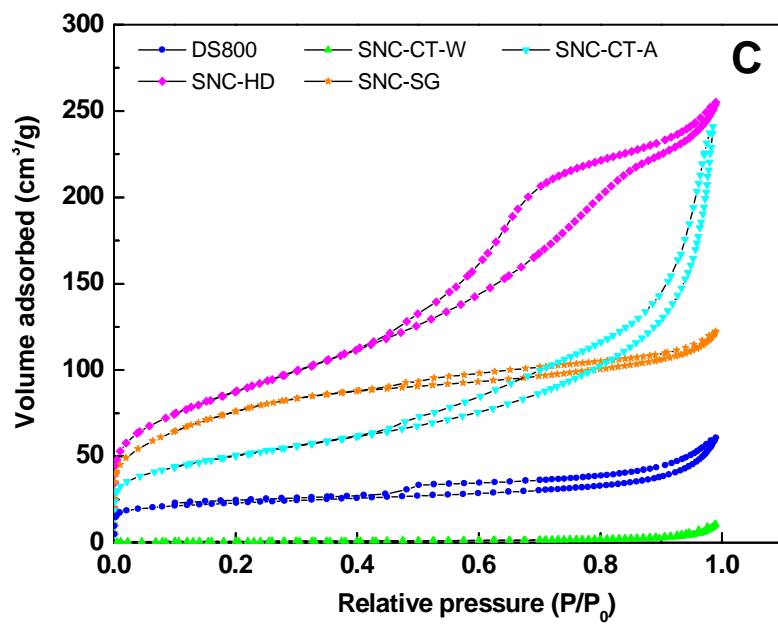
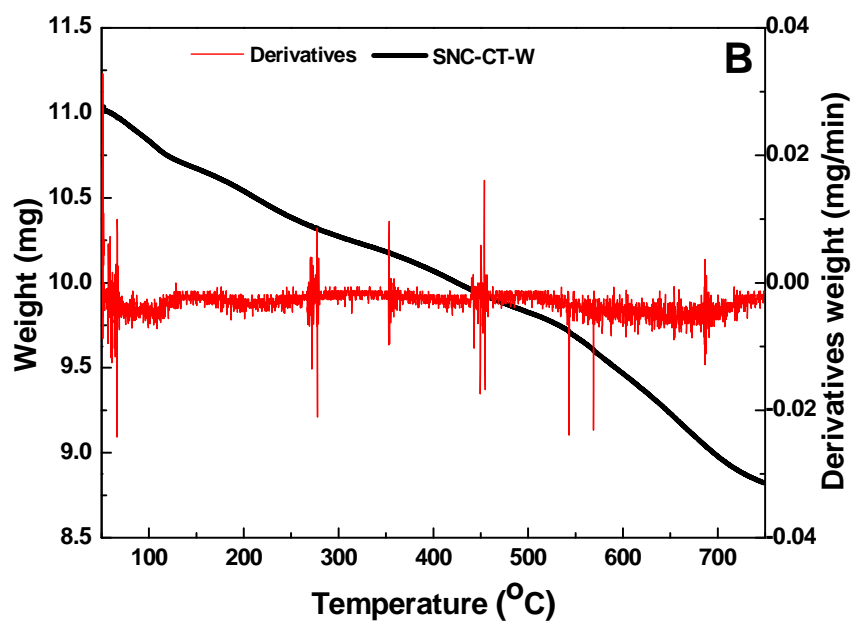
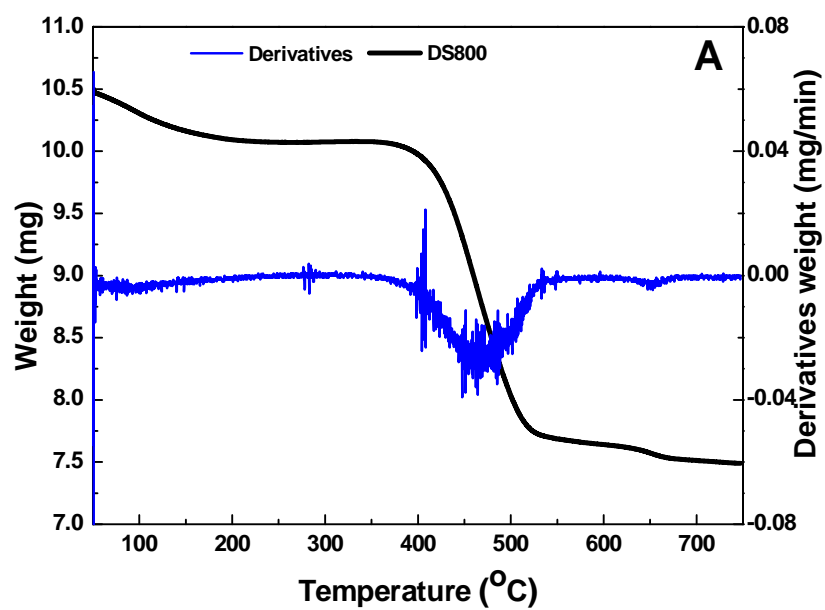
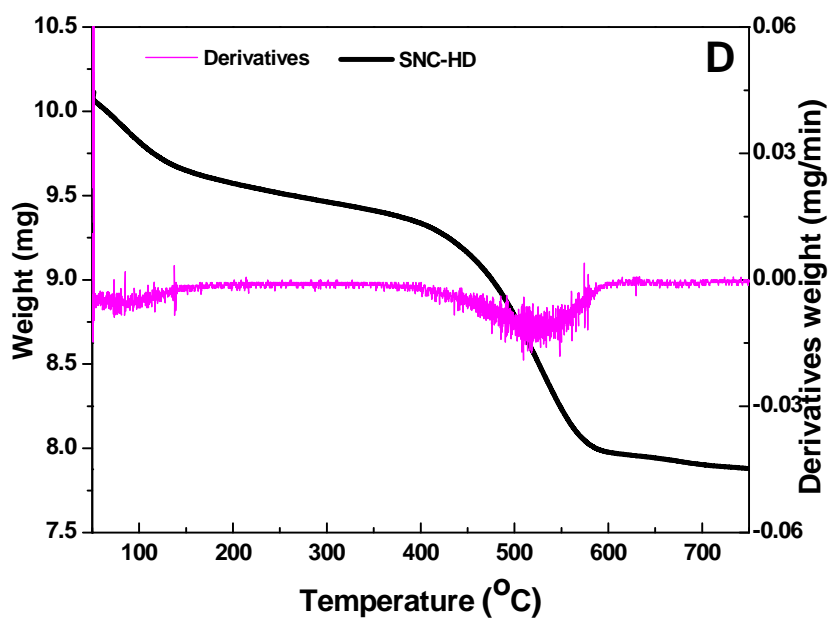
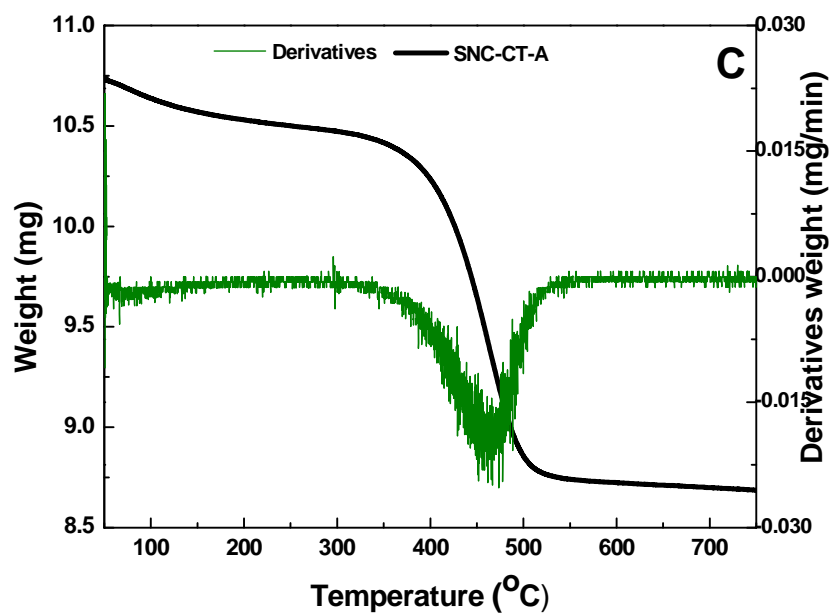


Figure 2.





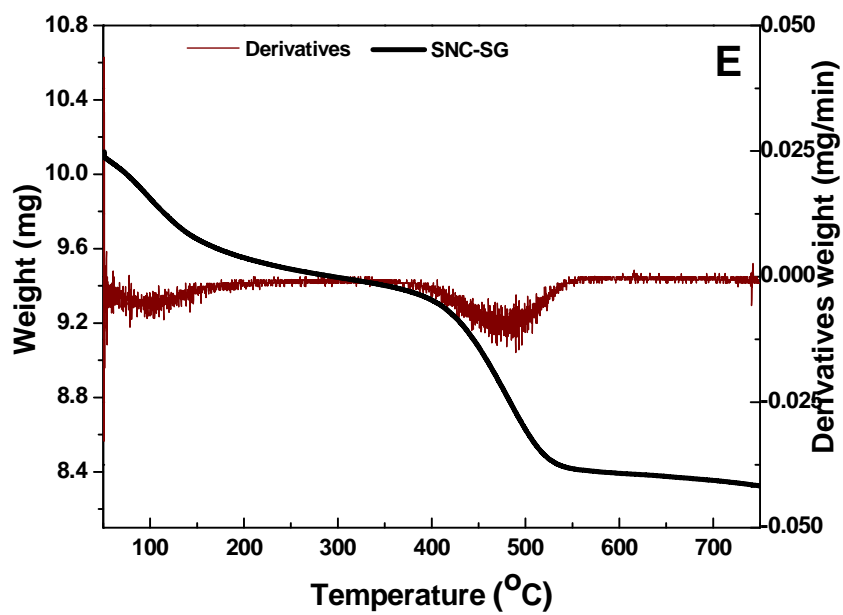


Figure 3.

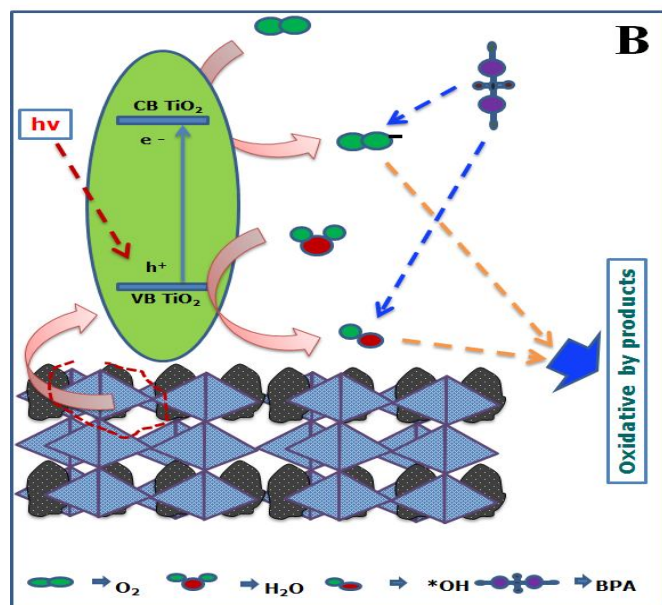
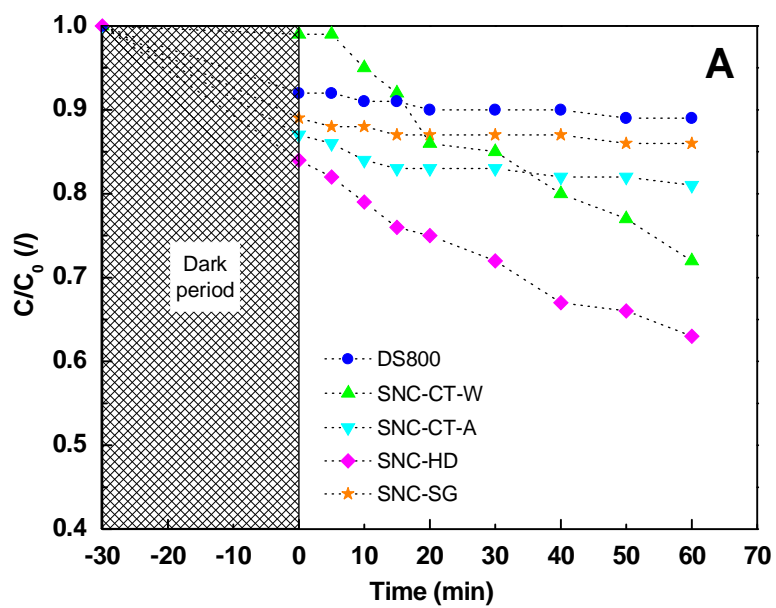
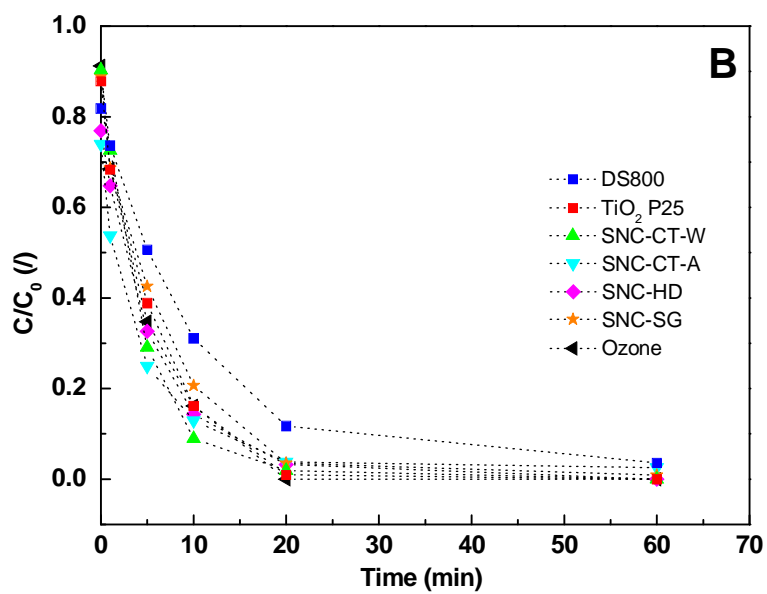
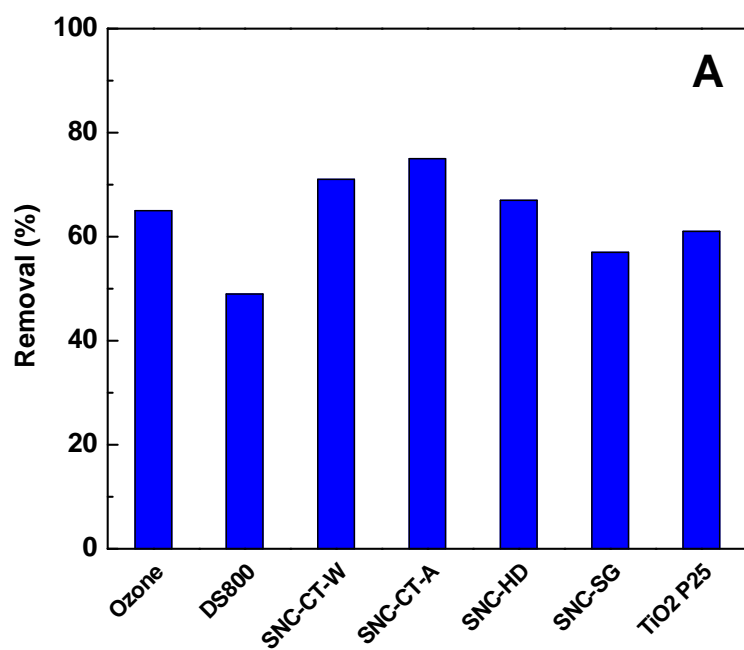
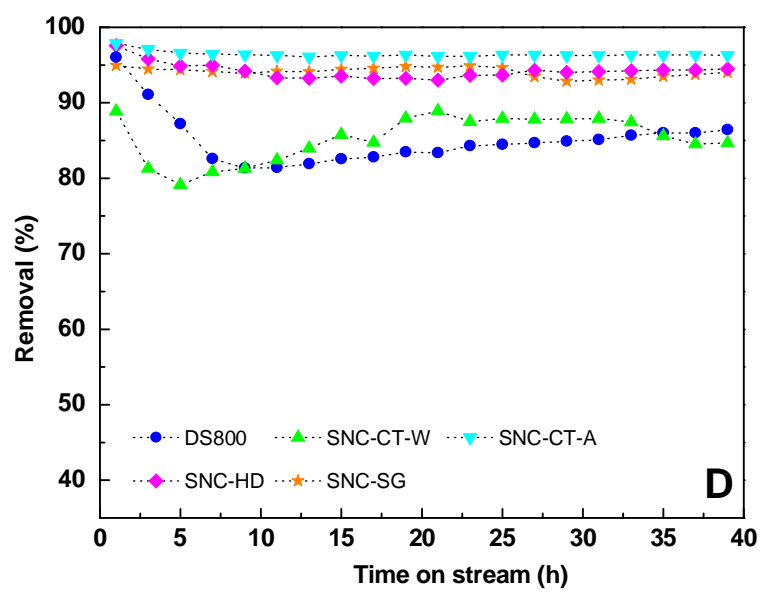
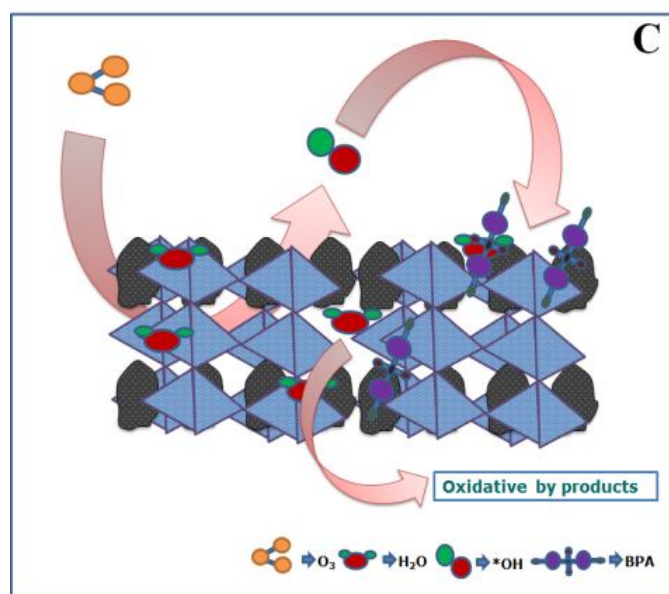


Figure 4.





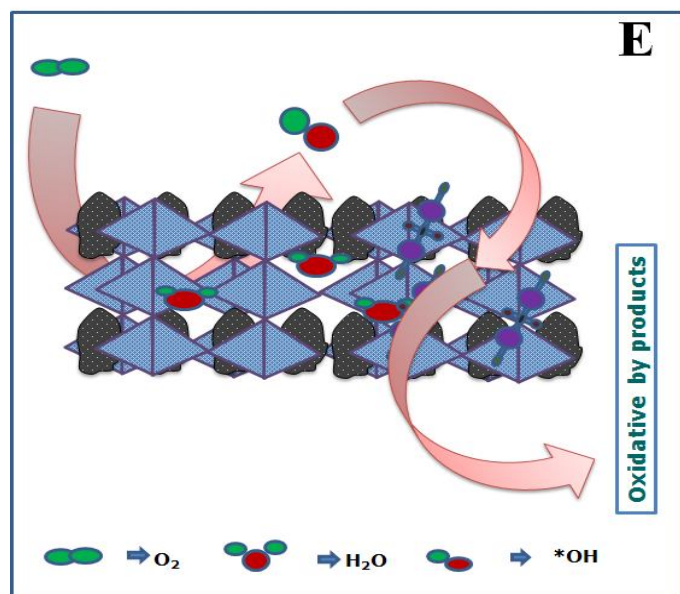


Figure 5.

TABLE CAPTION

Table 1. Specific surface area (S_{BET}), total pore volume (V_{pore}) and average pore width (d_{pore}) of sludge nano composites and DS sludge carbon.

Table 1

| Sample | S_{BET} (m^2/g) | V_{pore} (cm^3/g) | d_{pore} (nm) |
|----------|---|---|---------------------------|
| DS800 | 74 | 0.09 | 5.0 |
| SNC-CT-W | 3.0 | 0.01 | 22.1 |
| SNC-CT-A | 173 | 0.36 | 8.5 |
| SNC-HD | 309 | 0.39 | 5.1 |

| | | | |
|---------|-----|------|-----|
| SNC-SGS | 261 | 0.18 | 2.9 |
|---------|-----|------|-----|
